A novel method to produce a hierarchical porous carbon as a conductive support of PtRu particles. Effect on CO and methanol electrooxidation

Angélica M. Baena-Moncada [a,1], Gabriel A. Planes [a,*], M. Sergio Moreno [b,2], Cesar A. Barbero [a,*,1]

[a] Universidad Nacional de Río Cuarto, Ruta Nac. 36, Km 601 (X5804BYA), Río Cuarto, Córdoba, Argentina
[b] Centro Atómico Bariloche, 8400 − S.C. de Bariloche, Argentina

HIGHLIGHTS

► A novel and simple method for the synthesis of hierarchical porous carbon (HPC) is reported.
► The carbon present macropores and mesopores with large active surface area.
► Highly disperse PtRu nanoparticles are loaded inside the HPC by modifying the formic acid method.
► This hierarchical porous catalyst shows high activity toward methanol electrooxidation.

ARTICLE INFO

ABSTRACT

The fabrication and catalytic properties of hierarchical porous carbon loaded with PtRu particles was studied. A silica nanoparticles opal is filled with resorcinol/formaldehyde resin, which is then pyrolyzed to form a macroporous carbon. Depending on synthesis conditions the volume contraction induces mesopore formation in the macroporous carbon, creating a hierarchical porous carbon (HPC). The material consists of a thick, highly porous electrocatalytic film. PtRu nanoparticles were loaded inside the HPC by reduction of metallic ions with formic acid. The electrocatalytic activity toward CO and methanol oxidation was evaluated. The current densities for methanol electrooxidation at 60 °C (220 $\mu A\ cm^{-2}$ and 120 Ag^{-1} at 0.55 V_{RHE}) reveals high activity, suggesting that the catalysts consist of well disperse, small PtRu nanoparticles, with a low degree of agglomeration and good accessibility for reactants.

1. Introduction

At present, PtRu catalysts are the most active for methanol oxidation [1]. Different electrode systems, such as electrochemical deposited Ru on Pt, bulk PtRu alloys and electrodeposited PtRu alloys, have been investigated extensively [2–7]. These studies have demonstrated that the presence of Ru on the electrode surface catalyzes the oxidation of CO species, and consequently, enhances the electrocatalytic activity for methanol oxidation and other fuels.

In previous papers [8,9], we had studied methanol electrooxidation on mesoporous (MP) Pt and Pt–Ru electrodes. Our earlier results suggest that this all-metal mesoporous catalysts are more efficiency than carbon supported PtRu thanks to the improved surface activity, which reach values as high as 0.82 A cm^{-2} for MPPt modified by adsorbed Ru (MPPt/Ru). In parallel, the results obtained by differential electrochemical mass spectrometry (DEMS) for these electrodes show that only half the current used during methanol electrooxidation produces CO_2.

In contrast, for carbon supported 20% Pt/Ru 1:1 (E-TEK) only CO_2 is detected (that is, conversion efficiency near 100%). However, the current densities obtained for such electrode are about 70 mA cm^{-2}. The difference in the catalytic activity toward the methanol oxidation is more than one order of magnitude.

Such difference is attributed to diffusion effects taking place in the catalytic film. Thick and compact films may induce high methanol conversion to CO_2 and low current densities due to:

1- The low (local) methanol concentration.
2- The richness of reaction subproducts, like formic acid and formaldehyde, which compete with methanol for the absorption sites.

On the other hand, thin films improve the diffusion of methanol and other soluble products by which:

1- The adsorption of formic acid and formaldehyde is low.
2- The methanol concentration at catalysts surface is high.

For the purpose of testing our hypothesis, carbon supported, high-porosity catalytic films are interesting because they can provide information about electrochemical reaction inside thick, but also extremely porous films, and the results can be compared to that obtained for thin mesoporous catalysts.

Hierarchical porous carbons (HPC) are very interesting carbon-based porous materials (PC) [10]. The materials are hierarchical because the materials have a multimodal porous size distribution, with each pore size contributing to the desired properties. Such materials could be obtained by the combination of different templates [11,12]. After impregnation with a carbon source (precursor) and solidification of the composite material, a heat treatment (pyrolysis) at high temperature (above 800 °C) in the absence of oxygen turns the precursor into carbon. Since precursor materials are organic polymers, containing hydrogen and oxygen besides carbon, the pyrolysis involve mass loss and volume contraction. Soft templates like polymers and surfactants are spontaneously eliminated during burning of the carbon material, and no post treatments are necessary for the pore voiding. On the other hand, hard templates like silica and metal oxides survive to high temperatures, and must be removed after pyrolysis by chemical etching. In this process, the space initially occupied by the templates is transformed into the pores in the resulting carbon materials. The whole process results in a reverse copy of the template [13].

In this paper, it is shown that pyrolysis of a resin which mimics a hard template structure produces a carbon material with both macro and mesoporosity. While the macropores are due to the template effect of the hard silica spheres, the mesoporosity seems to be related to the cracks produced in the carbon due to restricted contraction. In the best of our knowledge, this effect has been used here for the first time to produce hierarchical carbon materials. To test such hypothesis, the template was also removed before pyrolysis and both materials were compared.

Finally, PtRu nanoparticles were loaded (20% w/w) on the hierarchical porous carbon (HPC−Pt/Ru). Using this electrode material, we produce thick, but also highly porous electrocatalytic films. The catalytic activity of the thick films produced with (20% w/w) (HPC−Pt/Ru) was evaluated toward CO and methanol electrooxidation, and the results compared with those previously reported for mesoporous PtRu and commercial catalysts PtRuC (20% w/w E-TEK).

2. Experimental

2.1. Synthesis of the HPC

In the present study, HPC is synthesized by a hard template approach, using SiO_2 nanospheres as template agent. The SiO_2 nanoparticles of 400 nm in diameter were synthesized by TEOS hydrolysis in basic media [14], and further used as templates. With this aim, SiO_2 nanoparticles were deposited by sedimentation in the bottom of a vial [15].

After solvent evaporation, the resulting weak opal was taken out of the vial and then treated at 1000 °C for 4 h to form a connected matrix of SiO_2 nanospheres. The template was then impregnated by the carbon precursor, a mixture of resorcinol (1 g), formaldehyde (1.6 ml), and sodium carbonate (0.4 ml, 0.1 M) as catalyst. The impregnated SiO_2 opal was dried in an oven and polymerized at (105 °C) to obtain a resin (RF) containing the silica nanospheres.

With the purpose of studying the effect of the template removal on carbon porosity, the SiO_2 of a sample was removed before

pyrolysis by treatment with hydrofluoric acid solution (*sample A*). The porous resin material was then pyrolyzed into carbon. Another sample, denoted as *sample B*, was pyrolyzed in the presence of the SiO_2 template. The pyrolysis of both samples was carried out at 850 °C for 24 h. The morphological characterization was performed using SEM and HRTEM.

2.2. Electrochemical characterization of the HPC support

Cyclic voltammetry was carried out to measure the electrochemical active area of both samples. An electrochemical evaluation of the carbon area has been preferred here due our interest in using these materials as supporting materials for fuel cell catalysts [16], but also in other electrochemical devices for energy production and storage [15] like electrochemical double layer capacitors [17,18] and carbon/graphite composed materials for Li ion batteries [19,20].

This measurement gives an accurate idea of the accessible surface for any electrochemical process in aqueous media.

The differential capacitance was calculated as:

$$Cd = i(A)/v(Vs^{-1})$$

With aid of this formula, current in the CV can be expressed as differential capacitance. Capacitance gives a comparative idea of the extension of the electroactive area. The straight conversion to capacitive values has been possible due to the insignificant pseudocapacitive (faradaic) contribution shown by the surface (see below).

2.3. HPC impregnation with PtRu

The HPC (*sample B*) was loaded (20% metal) with Pt/Ru nanoparticles using a variation of the formic acid method [21]. Due to the nature of the material to be impregnated, a porous solid with particle size around 25 μm, the order in which reactants are added to the carbon suspension was modified. In the conventional method, the last step involves the addition of the metallic precursors to be reduced. However for the porous carbon microparticles, the metallic precursors must reach the nanoparticle cores before beginning of the reduction. This last process is slow, because the precursors must pass through to the porous structure and reach the core of the carbon microparticle assisted only by diffusion. For this reason, the first step here is the addition, under vigorous stirring, of metal precursors to the HPC. This mixture is keeping under stirring for 12 h, then the process is completed by the addition of an excess of formate solution (preceded by pH adjusting to 10). Finally, the HPC−Pt/Ru is washed with copious quantities of water, filtered and dried for its storage.

2.4. Electrochemical characterization. CO and methanol electrooxidation over HPC−Pt/Ru

The electrochemical experiments were carried out in a thermostatized three electrodes electrochemical cell, using a reversible hydrogen electrode in the electrolyte solution (RHE) as the reference. All potentials in this work are given against the RHE. A small piece of high surface carbon was used as auxiliary electrode. In this study, the working electrode consists of a certain amount of the HPC−Pt/Ru deposited as a thin layer over a glassy carbon disc (ϕ = 3 mm). For this purpose, an aqueous suspension of 4.0 mg mL^{-1} of the HPC−Pt/Ru catalyst was prepared by ultrasonically dispersing it in 15 μL of Nafion (5 wt.%, Aldrich) and pure water. An aliquot (20–50 μL) of the dispersed suspension was

pipetted on the glassy carbon surface and dried at ambient temperature under N_2 atmosphere.

Electrochemical measurements were performed in 1 M CH_3OH/ 1 M H_2SO_4 at 60 °C, with a PC controlled Autolab PGSTAT30 potentiostat–galvanostat and a thermostatized three electrodes electrochemical cell. We use a hydrogen reference electrode in the electrolyte solution (RHE) as the reference. All potentials in this work are given against the RHE. A small piece of high surface carbon was used as auxiliary electrode. Current densities J (A cm^{-2}) were calculated from the measured current I (A) and the real electroactive area S (cm [2]). S was estimated from the CO stripping experiments assuming a charge of 420 μC cm^{-2}. All reagents were of analytical grade. N_2 was bubbled through the solution to avoid dissolved oxygen. Methanol electrooxidation in was carried 1 M CH_3OH/1 M H_2SO_4 at 60 °C.

3. Results and discussion

3.1. Synthesis of the HPC

As we mentioned before, in this paper we explore a different approach for the simultaneous addition of mesoporosity to the macropore walls, the volume contraction of the carbon during pyrolysis. The volume contraction during pyrolysis of RF resin is easily observable by comparison between the piece size before and after thermal decomposition of the precursor, and amounts to 30–40% (w/w). However, when the carbon sample contains a rigid template, the observed contraction in the macroscale is very low due to the presence of a non compressible skeleton. In our case, this rigid support is composed by an array of nanometric SiO_2 nanoparticles in close contact between them. The SEM image of these SiO_2 nanoparticles (Fig. 1) reveals the existence of almost monodisperse spheres with diameter around 390 nm. The observed size agree with the results of the DLS experiments (not shown) which report SiO_2 NP diameter around 401 nm, with a polidispersity index of 0.0327 (~3%).

After impregnation, and once the resorcinol-formaldehyde resin have been cured, the rigid template can be eliminated, or preserved, during pyrolysis and dissolved later. The stage at which these rigid molds are eliminated defines, clearly, two different porous materials. The HRTEM image of sample A (Fig. 2) where SiO_2 were eliminated before pyrolysis, shows that this SiO_2 nanoparticles induce, in the carbon matrix, macropores with size range from 300 to 400 nm. An additional aspect to be noted is the

Fig. 1. SEM image of as-synthesized SiO_2 NP.

smoothness of the pore wall; the HRTEM image in Fig. 2 (inset, top and bottom) also shows that the pore wall of the sample A is clearly smooth and almost free of noticeable porosity.

In contrast, when the carbon is pyrolyzed in the presence of the SiO_2 template (sample B) a quite different material is obtained. The HRTEM image of the sample B (Fig. 3) shows a carbon skeleton composed of macropores (average diameter of ~400 nm) delimited by highly permeable mesoporous walls. A further increase in the magnification of the image shows that those porous walls are really composed of reticular carbon shapes (see inset in Fig. 3), with thickness of the carbon branches in the scale of ~10 nm. The carbon material so obtained shows a second level of porosity. This kind of nanostructures, namely sintered beads of carbon linked into a matrix through necks, has been proposed as the building block of RF resin, which after precipitation forms condensed monoliths [22,23]. In fact, carbon aerogels obtained by supercritical drying shows an identical structure in the mesoscale.

Note that the composition of polymeric precursor and the sample treatment is the same in both experiments until solidification of the RF resin inside the silica template. Thus, the interaction between the template and the polymeric precursor as the driving force responsible for different texture in the nanoscale level was discarded [24]. The difference in morphologies of the pore wall should not be a direct consequence of dissimilar condensation/ agglomeration of the RF sol inside the cavities of the SiO_2 templates, since this process is identical in both samples. However, it seems reasonable to assume that the existence of a high contact surface, in addition to the small volume of the RF network, can change the way in which RF nanoparticles agglomerates to copy the templates. However, in terms of stabilization, the expected result should be the inverse. Highly extended contact areas between RF and the SiO_2, present during pyrolysis, should promote the appearance of a smooth surface, mainly due to the additional stabilization of the RF precursor during the first step of carbonization.

We interpret this fact as follow. The mechanical strength and symmetry of the silica array prevents, to the RF precursor, of any local displacement or contraction on the macroscale. For this reason, the only functional mechanism for structural relaxation during pyrolysis operates over the pore wall dimension and, the most important fact; relax only short carbon domains. In this scale, the size reduction caused by the carbon densification results in a randomized disagglomeration of the sintered nanoparticles. The final result of the process is the formation of an interconnected carbon mesh, quite similar to that observed in aerogels. Nevertheless, a simple comparison between both HPC samples leads to conclude that the function of the templates largely exceeds the simplest patterning of the shape on the host structure.

While there are many interesting papers [25] and reviews [15,26] discussing strategies to generate HPC starting from a combination of multiple templates, the effect of contractions of materials and their potential to generate additional porosity at the nanoscale level has not been described until now.

3.2. Electrochemical characterization of the HPC support

Measurements of double layer capacitances give a semi-quantitative value for the electroactive area. When the SiO_2 template was removed after pyrolysis (sample B), the CV curve (continuous line in Fig. 4) shows high differential capacitance (130 F g^{-1} of carbon), associated with a large surface area. This capacitance value is quite similar to that reported before for the CMK type porous carbon [27]. From these values, a surface electroactive area around 700–900 m^2 g^{-1} can be roughly estimated (based on 15 μF cm^{-2}) [28]. However, if the SiO_2 template is removed after solidification of the resin-silica composite, but
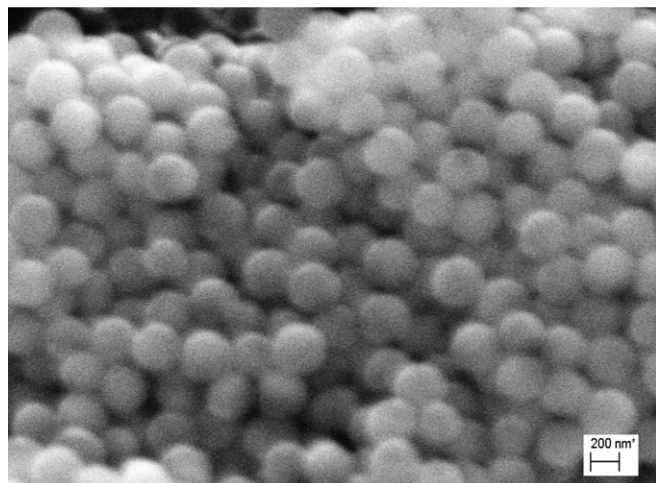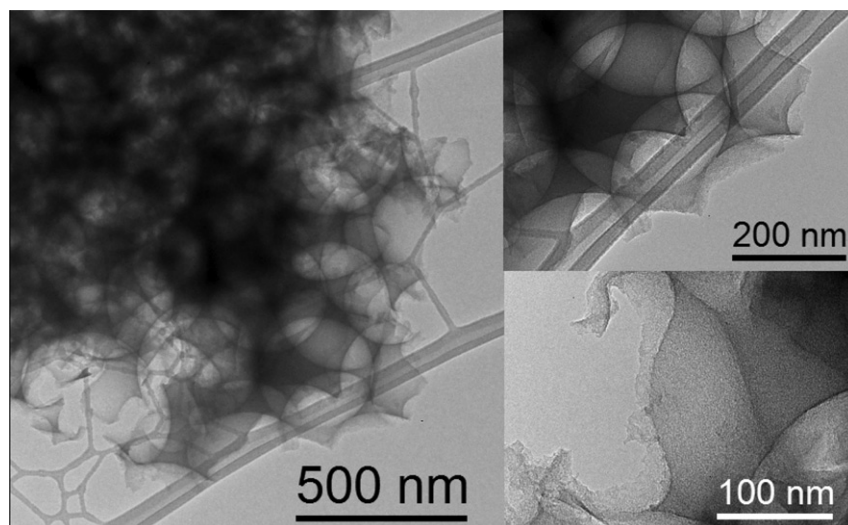
Fig. 2. HRTEM image of the PC obtained by RF pyrolysis performed after silica template removal from the RF (*sample A*). Inset (top), high magnification showing the macropore. Inset (bottom), high magnification showing the nanostructure of the pore wall.

before pyrolysis (*sample A*), the voltammogram shows a differential capacitance value of only 30 F g^{-1}, nearly a quarter of the other value (dashed line in Fig. 4). That disparity in differential capacity is in clear agreement with the observed carbon morphology. The inclusion of an additional level of porosity with size in the macroscale raises the accessible surface for the double layer formation. The capacitance is still large because the size of the silica spheres is still submicrometric.

As stated before, a straight conversion from current to capacitive values has been possible due to the insignificant pseudocapacitive (faradaic) contribution shown by the surface. In addition, the lack of pseudocapacitance shows that pyrolysis produce a material with low abundance of electroactive functional groups over the carbon surface [29].

Despite the fact that no definitive conclusion may be addressed about the causes of such extended surface area, the results shown here is in agreement with the existence of the additional porous sub-structure of the carbon wall. Note that one of the carbon samples, designated as *sample A*, was included in this work with the only purpose to clarify the effect that the presence of the hard template has on the resulting porous structure. Due to its negligible mesoporous area, its usefulness as electrocatalytic support for Pt/RuNP should be very low and it is not studied in this paper.

3.3. HPC impregnation with PtRu

With the aim of testing the utility of the HPC as support for catalysts, a sample of HPC (*sample B*) was loaded with 20% (w/w) of Pt/Ru (1:1) as described in the Experimental section. The election of *sample B* as support for PtRu NP was preferred because the high porosity and hierarchical nature of the porous structure makes this material the best candidate to test the hypothesis.

The HRTEM image of the HPC–PtRu (Fig. 5) shows good nanoparticle dispersion, with nanoparticle size around 2 nm. We also tested the formic acid method without further modification [21], but our preliminary results (not shown here) suggest that the straight application of the method produces very low mass activity toward methanol electro-oxidation, probably due to PtRu nanoparticle agglomeration in the outer surface of the HPC
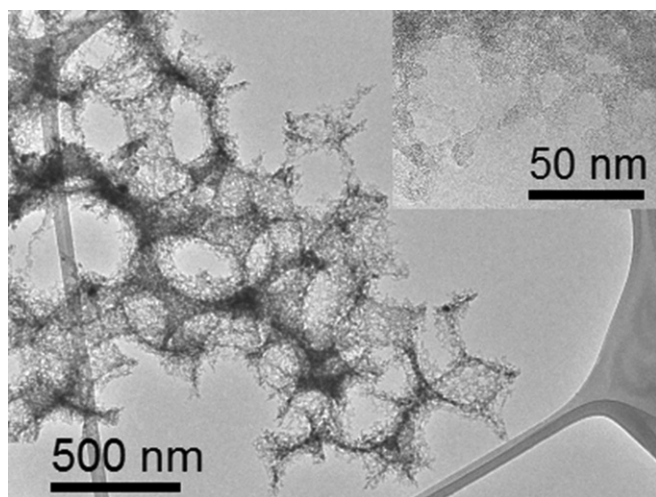

Fig. 3. *Principal*, HRTEM image of HPC obtained by RF pyrolysis in presence of silica template (*sample B*), followed by removal of the template. Inset, high magnification showing the nanostructure of the pore wall.
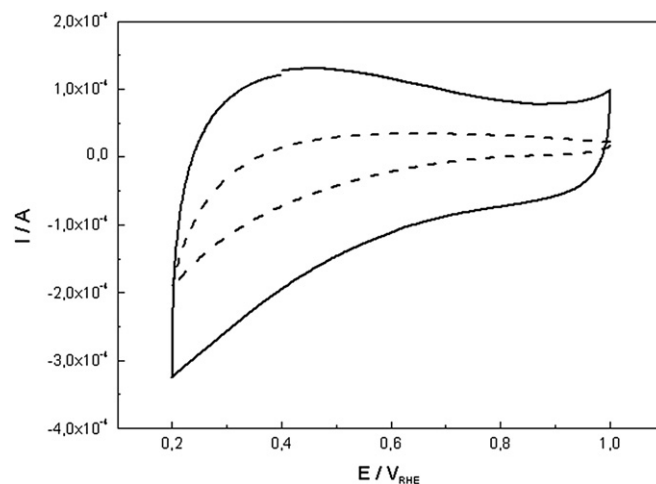

Fig. 4. Cyclic voltammogram of HPC obtained by RF pyrolysis in presence of the silica template (continuous line) and in his absence (dashed line).
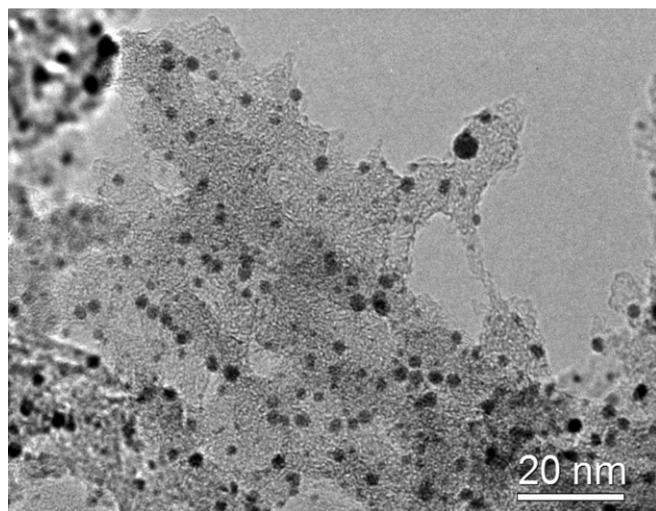
Fig. 5. HRTEM image of HPC (denoted as *sample D*). Obtained as stated before for *sample B*, and later loaded with PtRu.

microparticle. Nevertheless, these results are under study and will be subject of a further publication. The EDS analysis (not shown) performed at the HPC−Pt/Ru give a metal relationship Pt to Ru of 0.88 (47% Pt and 53% Ru), while the element mapping over a catalyst microparticle shows a uniform distribution of both elements.

3.4. HPC−Pt/Ru film characterization

A thick film of HPC−Pt/Ru/Nafion was deposited over a smooth glassy carbon electrode by casting method, as described in the Experimental section. The film so obtained shows a thickness around 11 μm, as can be observed by inspection of the SEM image of the deposit (Fig. 6, principal). The SEM image shows that the film has a homogeneous and very porous structure. Noteworthy, the film thickness (around 11 μm) is lower than the average HPC microparticle size (∼25 μm).

The homogeneity observed in all the films studied here suggests that the size of the HPC microparticles integrated in the film is smaller than the initial size. The particle size reduction might be caused by the action of the ultrasonic bath in two stages, first during impregnation, and later during the ink preparation. Even more, in some peripheral region of the electrode can be observed

Fig. 6. *Principal.* SEM image of a HPC−Pt/Ru film section. Inset, small structures composed of broken carbon meshes observed at the peripheral region of the electrode.

small structures composed of broken carbon meshes (inset in Fig. 6). Probably these very small carbon units are responsible of the inter-particle filling.

3.5. HPC−Pt/Ru electrochemical characterization. CO and methanol electrooxidation

The film so obtained was tested as electrode toward CO and methanol electrooxidation. The cyclic voltammogram in clean, O_2 free 1 M H_2SO_4 electrolyte (black dotted line in Fig. 7) shows the characteristic features of carbon supported Pt/Ru materials [30].

Looking for a more exact characterization of the catalyst surface, CO stripping experiments were performed at two different temperatures, 25 (black dash line) and 60 °C (black solid line). The adsorption was performed by exposition of the electrode to a CO saturated solution (10 min), keeping the electrode potential fixed at 0.25 V. After that, clean electrolyte (CO free) was flushed for additional 20 min in presence of bubbling N_2, to prevent the existence of dissolved CO during the stripping. One of the most important information that can be extracted from CO striping experiments is the real electroactive area of the catalysts. The electroactive surface area (ESA) of the HPC−Pt/Ru is 21.82 cm^2 (calculated assuming 420 μC cm^{-2} for CO stripping). Considering that the film contains 40 μg of the catalysts, the calculation gives approximately 54 m^2 g^{-1} of Pt/Ru. This value is reasonable for small and highly distributed PtRu nanoparticles.

As can be deduced from a simple inspection of Fig. 7, the presence of Ru shifts the onset and the peak position of the CO electrooxidation toward more negative potentials, when compared with Pt [8,9]. An increasing of the temperature from 25 to 60 °C produces a significant (0.1 V) peak displacement in the cathodic direction, from 0.56 to 0.45 V. The peak position and his dependence with temperature are in good agreement with literature data [21]. The CO stripping voltammograms was also recorded with the commercial catalyst (PtRuC) at two different temperatures 25 °C (gray dash line) and 60 °C (gray solid line). The peak potential at 25 and 60 °C are situated at 0.56 V_{RHE} and 0.48 V_{RHE} respectively; while no substantial dependence of the onset for the CO oxidation (∼0.4 V_{RHE}) with temperature was observed for this catalyst. In addition, the shape of the CO oxidation peak turns to be more symmetric while the temperature increases.
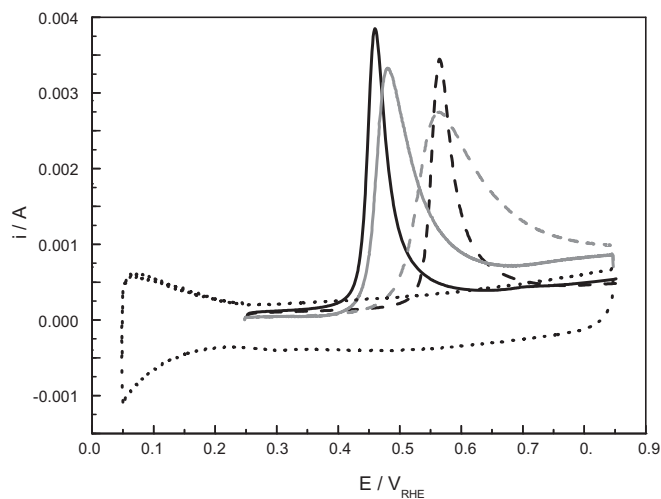

Fig. 7. CO stripping at 25 °C (dashed line) and 60 °C (solid line) for HPC−Pt/Ru (black line) and PtRuC (E-TEK gray line). CV in clean electrolite (dotted line). $E_{ad} = 0.25$ V, $t_{ad} = 10$ min. $v = 20$ mV s^{-1}.

An additional fact to be considered is the symmetry of the peak. The effect of sulfate anions on the shape of the CO striping peak is well known in literature. Sulfate anions adsorb strongly on Pt surface [31], blocking the CO diffusion toward the most active catalytic site. This fact produces peak asymmetry and long current tail. Interestingly, the HPC–Pt/Ru catalyst at 60 °C seems to be not affected by sulfate species, while only a small tail is observed at 25 °C.

The electrode activity toward methanol electrooxidation reaction (MOR) for MPC-Pt/Ru was also compared with the commercial PtRuC (E-TEK). The cyclic voltammetry in 1 M CH_3OH/1 M H_2SO_4 solution at 60 °C for both catalysts can be seen in Fig. 8.

The current density at 0.55 V HPC–Pt/Ru is close to 450 μA cm^{-2}, while the current at the peak (0.78 V) is 1.45 mA cm^{-2}. This values do not apart to match from those obtained for commercial catalysts like 20% (1:1) PtRuC (dotted line) [8]. Even more, the current density taken at 0.55 V is slightly higher for the commercial catalysts (∼550 μA cm^{-2}). The onset for MOR at 60 °C is positioned at 0.35 V, in good agreement with literature data [32].

An additional way to estimate the catalysts suitability for fuel cell applications involves chronoamperometric measurement of surface activity (A cm^{-2}) toward methanol oxidation. This technique provides additional information that not necessarily matches with that obtained by cyclic voltammetry, because the stationary character of the measurements intensifies some effects, like mass transport from/to solution, surface poisoning, and the appearing of CO_2 bubbles at the electrode surface. The response of the electrode to a potential step from 0.05 V (a potential where methanol adsorption and oxidation are negligible) to 0.55 V (a potential similar to that achieved during operation conditions in a fuel cell) can be observed in Fig. 9. In that condition, the current density reaches 220 μA cm^{-2} after 600 s of polarization. This value is higher than that measured for conventional carbon supported PtRu nanoparticles, and quite similar to that reported for mesoporous PtRu catalysts tested in the same conditions [8]. Expressed in terms of turnover frequency (TOF), this current density reach 0.52 s^{-1}. Assuming that three adsorption sites are required for each methanol molecule to be oxidized, this value implies that the whole catalyst surface is being renewed each 6 s.

As a criterion of metal utilization, the current can also be expressed in terms of mass activity. With this purpose, the obtained
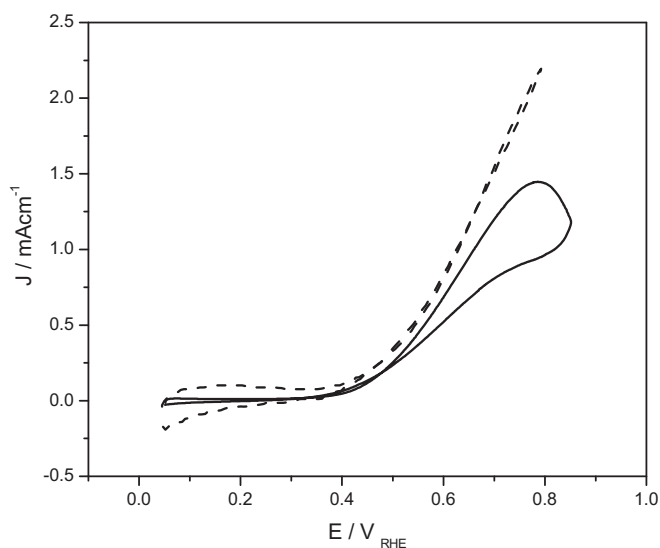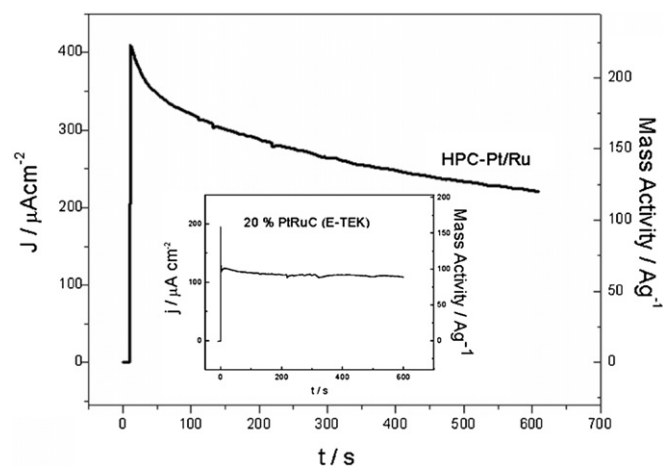

Fig. 9. *Principal*: current transients for methanol electrooxidation on HPC–Pt/Ru at 0.55 V_{RHE}, 1 M CH_3OH + 1 M H_2SO_4. T = 60 °C. Inset: current transients for methanol electrooxidation on PtRuC (E-TEK) at 0.55 V_{RHE}, 1 M CH_3OH.

current is divided by the total mass of the metal present at the electrode. This value is shown in the right axis of the Fig. 9. The obtained value after 600 s of polarization (120 Ag^{-1}, at 0.55 V_{RHE}) reveals that the catalysts consist of well disperse, small PtRu nanoparticles and low degree of agglomeration. As a reference, the inset in Fig. 9 shows the current transient obtained for the commercial PtRuC in similar condition of analysis (i.e. 0.55 V_{RHE}, 600 s of polarization, and 60 °C).

As we mentioned in the Introduction, the aim of the paper is to offer information about CO and methanol oxidation inside thick, but also extremely porous carbon films. The results of the electrochemical analysis suggest that the current density obtained from of a thick layer of HPC–Pt/Ru catalysts is very similar to that obtained for very thin (100–200 nm) mesoporous metal layer of PtRu, but quite different to conventional carbon-supported catalysts [33]. Although more studies are necessaries for corroborate the effect of porosity, thickness and mass transport inside catalysts layer, the result shown here suggests that high porosity and thick catalytic layers can follow the behavior of thin metal films.

4. Conclusions

In our best knowledge, the use of hard templates as indirect source of a second level of porosity has been described here for first time. These results show that it is possible to synthesize a useful and complex porous structures starting from a simple host matrix, i.e. double patterning by using a single template. The key factor is the fact that hard templates obstruct contraction, while soft templates (or its previous elimination) allow such contraction. This strategy can be used for reduction of time and efforts in the synthesis of complex hierarchical precursors.

The improved method for the metal impregnation provides a safe way to prevent metal agglomeration on the microparticle surface. Additionally, the existence of an interconnected macroporous network provides to the catalytic layer of multiple ways for methanol feeding and products release (i.e. CO_2, HCOOH and H_2CO).

The electrocatalytic activity expressed in terms of current density and mass activity support the idea of highly porous carbon matrix decorated with small catalysts nanoparticles, in good agreement with the previous characterization of the catalysts.

Finally, the normalized (Ag^{-1}) current performance of a thick layer of HPC–Pt/Ru catalysts is very similar to that obtained for extremely thin (100–200 nm) mesoporous metal layer of PtRu.

Fig. 8. CV at 60 °C in 1 M CH_3OH/1 M H_2SO_4 for HPC–Pt/Ru (solid line) and PtRuC (E-TEK dashed line). v = 20 mV s^{-1}.

Acknowledgements

References

[1] A.S. Aricò, S. Srinivasan, V. Antonucci, Fuel Cells 1 (2001) 133.
[2] G. García, J.A. Silva-Chong, O. Guillén-Villafuerte, J.L. Rodríguez, E.R. González, E. Pastor, Catal. Today 116 (2006) 415.
[3] G. García, V. Baglio, A. Stassi, E. Pastor, V. Antonucci, A.S. Aricò, J. Solid State Electrochem. 11 (2007) 1229.
[4] C.E. Lee, S.H. Bergens, J. Phys. Chem. B 102 (1998) 193.
[5] W.F. Lin, M.S. Zei, M. Eiswirth, G. Erh, T. Iwasita, W. Vielstich, J. Phys. Chem. 103 (1999) 6968.
[6] H.A. Gasteiger, N. Markovic, P.N. Ross Jr., E. Cairns, J. Phys. Chem. 98 (1994).
[7] Z. Jusys, H. Massong, H. Baltruschat, J. Electrochem. Soc. 146 (1999) 1093.
[8] G. García, J. Florez-Montaño, A. Hernandez-Creus, E. Pastor, G.A. Planes, J. Power Sources 196 (6) (2011) 2979.
[9] G.A. Planes, G. García, E. Pastor, Electrochem. Commun. 9 (2007) 839.
[10] J. Balach, M.M. Bruno, N.G. Cotella, D.F. Acevedo, C.A. Barbero, J. Power Sources 199 (2012) 386.
[11] Y. Deng, C. Liu, T. Yu, F. Liu, F. Zhang, Y. Wan, L. Zhang, C. Wang, B. Tu, P.A. Webley, H. Wang, D. Zhao, Chem. Mater. 19 (2007) 3271.
[12] Z. Wang, F. Li, N.S. Ergang, A. Stein, Chem. Mater. 18 (2006) 5543.
[13] B. Sakintuna, Y. Yürüm, Ind. Eng. Chem. Res. 44 (2005) 2893.
[14] W. Wang, B. Gu, L. Liang, W. Hamilton, J. Phys. Chem. B 107 (2003) 3400.
[15] O.D. Velev, A.M. Lenhoff, Curr. Opin. Colloid Interface Sci. 5 (2000) 56.
[16] B. Fang, J.H. Kim, M. Kim, J.-S. Yu, Chem. Mater. 21 (2009) 789.
[17] E. Frackowiak, F. Béguin, Carbon 39 (2001) 937.
[18] W. Xing, S.Z. Qiao, R.G. Ding, F. Li, G.Q. Lu, Z.F. Yan, H.M. Cheng, Carbon 44 (2006) 216.
[19] L. Shen, C. Yuan, H. Luo, X. Zhang, K. Xu, F. Zhang, J. Mater. Chem. 21 (2011) 761.
[20] Y. Wu, Z. Wen, J. Li, Adv. Mater. 23 (2011) 1126.
[21] W.H. Lizcano-Valbuena, V.A. Paganin, E.R. González, Electrochim. Acta 47 (2002) 3715.
[22] R.W. Pekala, J. Mater. Sci. 24 (1989) 3221.
[23] R.W. Pekala, C.T. Alviso, J.D. LeMay, J. Non-Cryst. Sol. 125 (1990) 67.
[24] W.W. Luken, G.D. Stucky, Chem. Mater. 14 (2002) 1665.
[25] A.F. Gross, A.P. Nowak, Langmuir 26 (2010) 11378.
[26] F. Ruo-wen, L. Zheng-hui, L. Ye-ru, L. Feng, X. Fei, W. Ding-cai, New Carbon Mater. 26 (2011) 171.
[27] F. Lufrano, P. Staiti, Int. J. Electrochem. Sci. 5 (2010) 903.
[28] X. Zhao, H. Tian, M. Zhu, K. Tian, J.J. Wang, F. Kang, R.A. Outlaw, J. Power Sources 194 (2009) 1208.
[29] B.E. Conway, Electrochemical Supercapacitors: Scientific Fundamentals and Technological Applications, Springer, 1999.
[30] J.R.C. Salgado, F. Alcaide, G. Álvarez, L. Calvillo, M.J. Lázaro, E. Pastor, J. Power Sources 195 (2010) 4022.
[31] A. Kolics, A. Wieckowski, J. Phys. Chem. B 105 (2001) 2588.
[32] J. Jiang, A. Kucernak, Electrochem. Commun. 11 (2009) 623—626.
[33] J. Jiang, A. Kucernak, Chem. Mater. 16 (2004) 1362.

Glossary

HPC: hierarchical porous carbon
MPPt: mesoporous platinum
MPPt/Ru: mesoporous platinum/rutenium
DEMS: differential electrochemical mass spectrometry
PC: carbon-based porous materials.
TEOS: tetraethyl orthosilicate
RF: resorcinol/formaldehyde resin
SEM: scanning electron microscopy
HRTEM: high-resolution transmission electron microscopy
RHE: hydrogen reference electrode
DLS: dynamic light scattering
CV: cyclic voltammetry
CMK: ordered mesoporous carbon
EDS: energy-dispersive X-ray spectroscopy
MOR: methanol electrooxidation reaction
TOF: turnover frequency